

ePIC LFHCal R&D Proposal - eRD107

Friederike Bock¹, Oskar Hartbrich¹, Nicolas Schmidt¹, Norbert Novitzky¹,
Constantin Loizides¹, Jacob Mireles¹, Ken Read^{1,6}, Ewa Glimos^{1,6}, Helen
Caines², Prakhar Garg², Fernando Flor², Iris D. Ponce-Pinto², Ananya Rai²,
Joshua Kerner², Zihui Zhang², Megan Connors³, John Lajoie⁴, Peter
Steinberg⁵, Craig Woody⁵, Brian Page⁵, Christine Nattrass⁶, Jim Freeman⁷,
Miguel Arratia⁸, and Adam Gibson⁹

¹*Oak Ridge National Laboratory, Oak Ridge, US*

²*Yale University, New Haven, US*

³*Georgia State University, Atlanta, US*

⁴*Iowa State University, Ames, US*

⁵*Brookhaven National Laboratory, Upton, US*

⁶*University of Tennessee, Knoxville, US*

⁷*Fermi National Laboratory, Batavia, US*

⁸*University of California, Riverside, US*

⁹*Valparaiso University, Valparaiso, US*

July 7, 2023

Version 1.1

1 Contents

| | | |
|----|---|-----------|
| 2 | 1 Introduction | 2 |
| 3 | 1.1 Requirements for the ePIC forward calorimeters | 2 |
| 4 | 1.2 Modified LFHCal and Insert Design | 3 |
| 5 | 2 R&D Progress FY23 | 5 |
| 6 | 2.1 Production of tiles | 5 |
| 7 | 2.2 Dark Box and Test Setup | 6 |
| 8 | 2.3 SiPM Characterization | 7 |
| 9 | 2.4 Optimization and Granularity of the LFHCal & Insert | 8 |
| 10 | 3 Remaining R&D Needs FY24 | 10 |
| 11 | 3.1 Scintillator Tiles | 10 |
| 12 | 3.2 Scintillator Characterization and Optimization | 10 |
| 13 | 3.3 Readout Electronics | 11 |

| | | | |
|----|----------|---|-----------|
| 14 | 3.4 | Prototypes and Test beams | 11 |
| 15 | 3.5 | Optimization of the Reconstruction Algorithms & Granularity of the LFHCal . . | 12 |
| 16 | 4 | Plans and Milestones for FY24 | 12 |
| 17 | 4.1 | Money Matrix | 13 |
| 18 | 5 | Plan for FY25-26 | 13 |
| 19 | A | Appendix | 15 |
| 20 | B | Detailed Funding Allocation for R&D in FY24 | 15 |
| 21 | B.1 | Specific Expertise of Contributors | 16 |
| 22 | B.1.1 | Oak Ridge National Laboratory | 16 |
| 23 | B.1.2 | Brookhaven National Laboratory | 16 |
| 24 | B.1.3 | Fermi National Laboratory | 16 |
| 25 | B.1.4 | Georgia State University | 17 |
| 26 | B.1.5 | Iowa State University | 17 |
| 27 | B.1.6 | University of Tennessee Knoxville | 17 |
| 28 | B.1.7 | Yale University | 18 |
| 29 | B.1.8 | University of California, Riverside | 18 |
| 30 | B.1.9 | Valparaiso University, Valparaiso | 18 |

31 **1 Introduction**

32 **1.1 Requirements for the ePIC forward calorimeters**

33 In electron-proton (ep) or electron-ion (eA) collisions, many highly-energetic hadrons are cre-
34 ated in the process of probing the partonic structure of the target proton or ion using the
35 electron. However, since the incoming proton/ion has a significantly larger kinetic energy
36 than the incoming electron, most of the hadrons are emitted in the same direction as the
37 hadron beam, into the hadron end cap, which is defined as the "forward" direction at the
38 EIC. Thus jets of particles, with single-particle energies of up to 150 GeV, are expected to reach
39 the forward hadronic calorimeter, e.g. based on simulated PYTHIA events for ep collisions at
40 18×275 GeV². Typical jets consist of 10-12 particles contained within a jet radius of $R = 1$,
41 with R being the angular distance $\sqrt{\eta^2 + \phi^2}$. These jets also contain nontrivial substructure
42 within this cone, which carries important information about QCD dynamics. Unfortunately,
43 the tracking momentum and angular resolution worsens rapidly above $\eta = 3$. Because of
44 this, the hadronic and electromagnetic calorimetry in that region are required to provide both
45 excellent energy resolution and sufficient spatial resolution to resolve particles within the jets.
46 Thus, the forward calorimeter system has to be finely-segmented and built with minimal dead
47 space between the towers. This design will provide shower containment for highly energetic
48 particles while still providing good energy resolution down to low energies. The R&D for
49 the hadronic calorimeter will be coordinated within this eRD project, while the developments
50 for the ePIC forward electromagnetic calorimeter (known as pECal) are being carried out in
51 eRD106.

1.2 Modified LFHCal and Insert Design

The ePIC forward HCal (LFHCal) will be based on a longitudinally-segmented steel-scintillator tower design with a tungsten-scintillator collimator section (modified design based on [1]). The design is based on the SiPM-on-tile concept first introduced by CALICE collaboration [2], which is now being further developed for the CMS HGCAL upgrade [3]. It has been adapted to satisfy the physics performance requirements of the EIC Yellow Report [4] and will include an insert surrounding the beam pipe with even higher granularity readout following the same general concept.

The LFHCal is positioned at $z = 3.58$ m from the interaction point, and is preceded by the inner tracker and PID detectors as well as the pECal. The calorimeter is comprised of two half-disks with an outer radius of about 2.7 m.

The LFHCal towers have an active depth of $\Delta z = 1.3$ m with an additional space for the readout of about 10 cm, as summarized in Table 1. Each tower consists of 65 layers with alternating layers of about 1.6 cm absorber and 0.4 cm scintillator, with transverse dimensions of 5×5 cm². The first

4 absorber layers, after the steel front plate, consist of tungsten, followed by 60 layers of steel absorber. The tungsten layers act as a collimator for the initial shower and enable a maximization of the hadronic interaction length within the available space.

The towers are constructed in units of 8- and 4-tower modules, to ease the construction and reduce the dead space between the towers. Each scintillator tile (5 cm \times 5 cm \times 0.4 cm) is individually wrapped in reflective foil and then sheets of 2×4 or 2×2 tiles are assembled for each layer of the 8M or 4M modules respectively. These tile assemblies consist of a layer of kapton tape on the top and bottom for stability, the wrapped scintillator tiles and a flexible PCB carrying the SiPMs and an LED system for monitoring purposes, see Figure 1 top center. The flexible PCBs are connected to a long carrier PCB on one side of the module, which transfers the electrical signals from each individual tile to the back of the calorimeter. In order to reduce the number of readout channels within each tower SiPM signals from the first 5 tiles, and 10 tiles thereafter, are combined using an intermediary summing board at the back of the calorimeter. These signals are then processed by an ASIC based on the CMS HGCROC chip [3].

For the majority of the calorimeter we will be using SiPMs with an active area of 1.3 cm \times 1.3 cm (ie. Hamamatsu S13360-1325PE or S14160-1315PS) and injection molded scintillator tiles. However, in the current design neither the scintillator tiles nor the SiPMs can be accessed after the calorimeter has been assembled for radii below 1 m we are therefore considering using larger SiPMs with an area of 3 cm \times 3 cm (ie. Hamamatsu S13360-3025PE or S14160-3015PS) together with cast and machined scintillator tiles to mitigate the expected radiation damage. The full LFHCal consists of 62 414 readout channels grouped into 8916 tow-

| parameter | LFHCal |
|-------------------------|--|
| inner x, y | 60 cm |
| outer radius (envelope) | 270 cm |
| η acceptance | $1.2 < \eta < 3.5$ |
| tower information | |
| x, y | 5 cm |
| z (active depth) | 130 cm |
| z read-out | 10 cm |
| # scintillator plates | 65 (0.4 cm each) |
| # absorber sheets | 61 (1.52 cm steel) 4 (1.52 cm tungsten) |
| interaction lengths | $6.5 \lambda / \lambda_0$ |
| Sampling fraction f | 0.035 |
| # towers | 8916 |
| # modules | |
| 8M | 1077 |
| 4M | 75 |
| # read-out channels | $7 \times 8916 = 62,414$ |

Table 1: Overview of the calorimeter design properties for the LFHCal.

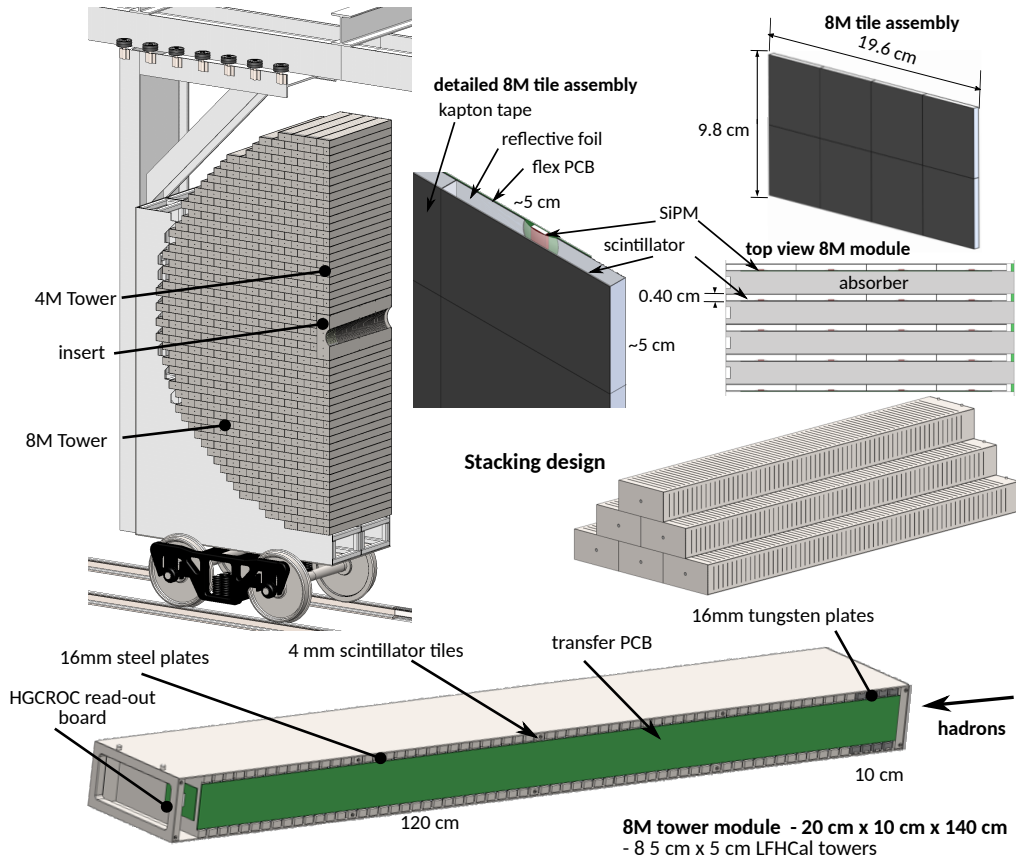


Figure 1: Renderings of the forward calorimeter assembly (top left), tile assembly of 8 scintillator tiles of the LFHCal with the SiPMs sitting in a dimple on each tile, detailed stacking example (middle right) and 8-tower module design (bottom).

98 ers. The majority of the calorimeter is built of 8-tower modules (~ 1077) which are stacked in
 99 a support frame using a "lego"-like system for alignment and internal stability. The remain-
 100 ing 4M modules are necessary to fill the gaps at the edges to allow for maximum coverage.
 101 It is complemented with an insert surrounding the beam pipe $60\text{ cm} \times 60\text{ cm} \times 140\text{ cm}$ using
 102 the same technology and absorber geometry. By using asymmetric and layer by layer varying
 103 cutouts around the beam pipe radius the coverage can be increased up to $\eta \approx 3.8$. This inlay
 104 will also serve as internal support structure around the beam-pipe for the LFHCal.
 105 The internal structure of the 8M modules is as follows. The absorber plates in the modules
 106 are mounted to the sheet metal frame using e-beam welding on three sides, keeping them in
 107 place while adhering to the tolerances and providing internal stability. On the left side of each
 108 module, a channel is left for installation of the scintillator sheet assemblies and the transfer
 109 PCB, which is afterwards closed with a cover to protect the electronics, as can be seen in Fig-
 110 ure 1 (bottom). For internal alignment we rely on the usage of 1 – 2 cm steel pins at the end
 111 of each module which are directly anchored to the back plate and a bolt in the front which is
 112 mounted to a continuous steel plate covering the front face of the calorimeter. This steel plate
 113 simultaneously serves as support plate for the forward ECal. Consequently, the modules are

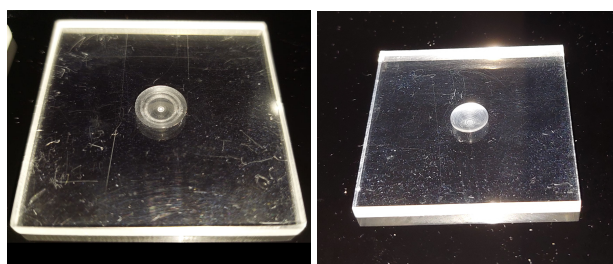


Figure 2: Picture of machined tiles with different machining procedures. Left: Tiles cut with water jet. Right: Tiles cut with modified wet tile saw. Dimples extruded using ball nose end mill.

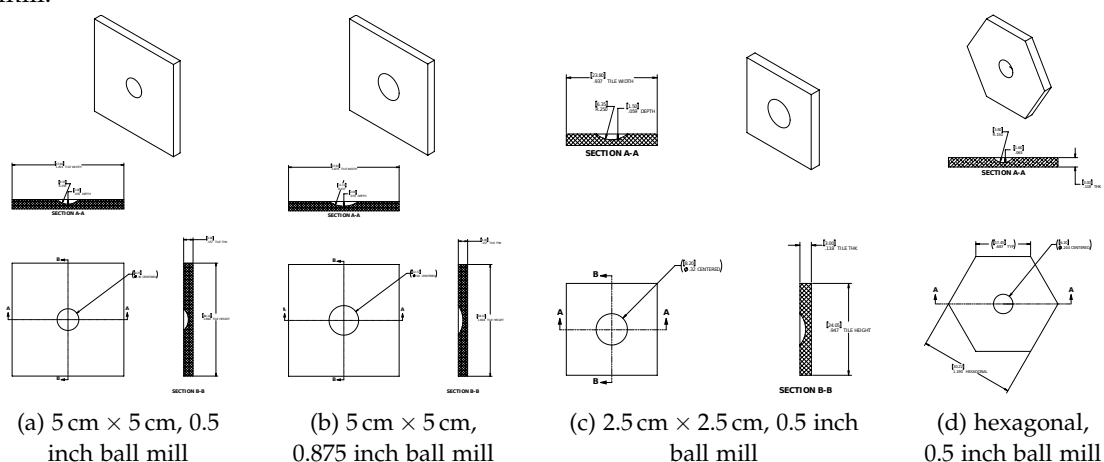


Figure 3: Tile models to be injection molded using the same mold.

114 self-supporting within the outer support frame.

115 The support frame for the half disks is arranged on rails which allows the HCal and ECal
 116 to slide out to the sides and gives access to the inner detectors. In addition, the steel in the
 117 LFHCal serves as the flux return of the central 1.7 T magnet. As a consequence, a significant
 118 force is exerted on the calorimeter, which needs to be compensated for by the frame and
 119 internal support structure.

120 2 R&D Progress FY23

121 2.1 Production of tiles

122 After receiving the R&D money for FY23 in March 2023 at ORNL, we conducted a market
 123 survey for obtaining cast and machined scintillator material from different vendors. The most
 124 promising vendors for the cast material are Eljen and Luxium Solutions. Both vendors are
 125 able to provide the cast material with similar light yield for 60K tiles within one year. Their
 126 machining capabilities and prices are however very different. As such, several studies have
 127 been conducted at ORNL on how the machining of these delicate materials could be done for
 128 large quantities. An example of the first attempt carried out by the ORNL machine-shop can

129 be found in Figure 2 (left). The machining was done using a water jet cutter with the standard
130 settings for plastics. As can be clearly seen the material is too sensitive to be handled in this
131 manner resulting in cracks at the outer edges. The dimple was extruded with a ball nose
132 end mill, which had been used prior to this for other materials. This lead to scratches in the
133 material.

134 With the help of our local scintillator expert Michael Febbraro the procedures for the different
135 steps were improved leading to significantly improved production results. The tiles are cut
136 using a modified wet tile saw (i.e. RIDGID 9) with the protective foil still attached. The speed
137 of the tile saw is decreased to about 10-30% of the factory setting by running it off a variac and a
138 higher volume water pump is used to increase the cooling. Using this setup a current precision
139 of 1.5 mm can be achieved on the outer edges. This could be further improved by creating a
140 more precise rig for the tiles to be held by. Only distilled water is used as the cooling solution
141 to avoid crazing due to chemical interactions. Afterwards the exact dimensions are reached
142 using a fly cutter. This can be done for multiple tiles at once. During this whole process the
143 protective foil is left in place. Only for cutting the dimple it is removed on the top. Similar
144 to the ORNL machine shop the dimple was created using a ball nose end mill, however the
145 process was significantly slowed down and cutting tool was only used for scintillator materials
146 before. Afterwards, the dimple and edges were polished using a buffing wheel combined with
147 a tiny drop of unscented Dawn-soap, 0.3μ Alumina power and water. This improved procedure
148 resulted in significantly better quality tiles. Nonetheless, minor scratches on the surface arising
149 from handling and dust particle are visible in Figure 2 (right). Estimates by the expert suggest
150 that in a production setup 200-300 tiles could be cut per hour. The drilling and polishing of
151 the dimples could be achieved with a rate of about 150-200 tiles per hour.

152 In parallel we have asked Eljen an Luxium to produce some test samples of the final product
153 and we are waiting to receive them to test their production quality. An order of 600 tiles
154 provided by Eljen should be received before the parasitic test beam at CERN in September
155 2023.

156 In parallel to the machining efforts a mold for injection molding four different tile types has
157 been ordered by Fermilab recently. Within this mold during one inject one tile of each type
158 will be produced. Two of these tiles correspond to the standard LFHCal tile sizes but different
159 dimple geometries, while the other two are being evaluated for use in the insert. Compared
160 to the cast scintillator, we are expecting about 30% reduced light yield, as seen in previous
161 experiments. However, the production tolerances are significantly better and the tiles can be
162 produced at a reduced price as well as in a shorter amount of time. Using the first samples
163 using our mold we will try to optimize the tile geometry as well as production mechanisms
164 using injection molding, similar to what has been done for the machining within this R&D
165 program.

166 2.2 Dark Box and Test Setup

167 Two different light-tight dark boxes were designed and assembled at Yale and ORNL, respec-
168 tively. They feature a panel with throughputs for SMA, SHV, 20 pin headers, and banana
169 connectors and a door or removable panel for easy access to the setup inside as shown in
170 Figure 4(a). The dark box is also a Faraday cage that shields external interference, in turn
171 allowing for investigation into intrinsic properties of the SiPM's, and the characterization of
172 both the SiPM's and scintillation tiles.

173 PCB boards holding a SiPM as shown in Figure 4(b) are used for testing and characterizing

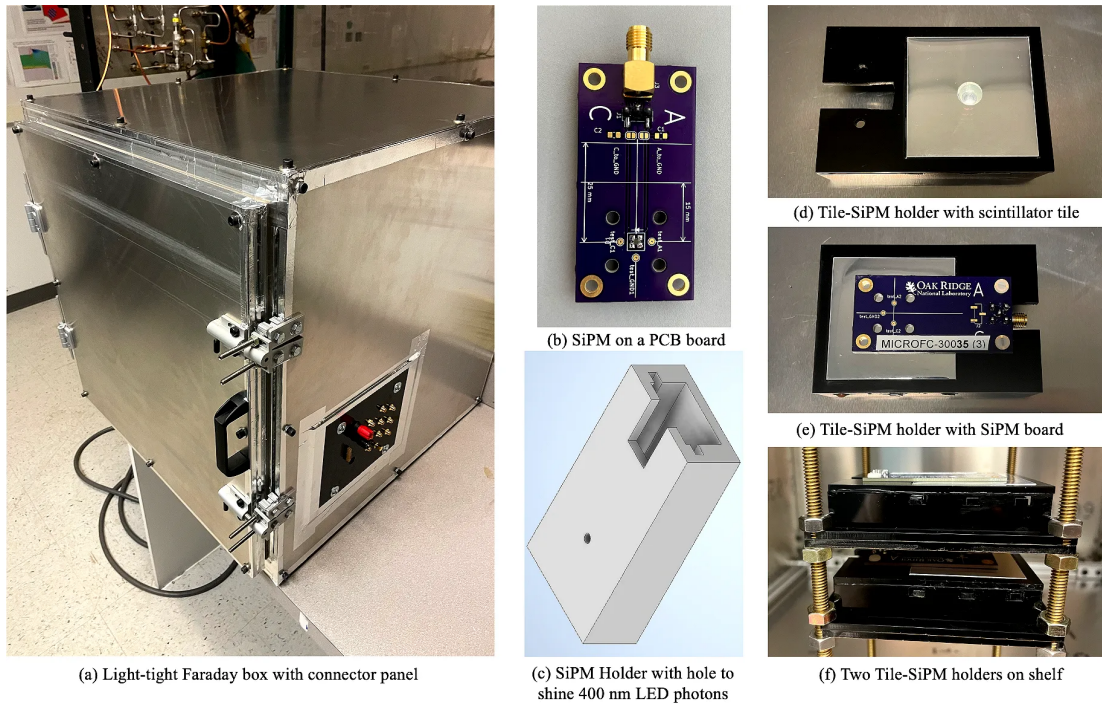


Figure 4: (a) Setup to provide a light-tight environment for testing the SiPM's including a light-tight box with a panel with throughputs for connectors at Yale, (b) SiPM on a PCB board, PCB board holder with a hole for an LED pulser for single photon efficiency tests, (c) a Tile-SiPM holder that holds the SiPM and tile together and aligned during testing (d and e), and a shelf with slots holding the Tile-SiPM holders at different distances for coincidence tests.

174 the scintillator tiles for the LFHCal. The functionality of the SiPM's were tested using an LED
 175 pulser that was held vertically above the SiPM chip using the SiPM PCB holder shown in Fig-
 176 ure 4(c).

177 For future coincidence tests, Tile-SiPM Holders with the PCB boards screwed for stability were
 178 created as shown in Figure 4 (d) and (e).

179 2.3 SiPM Characterization

180 Silicon Photomultipliers (SiPM's) are produced by various vendors in different packaging and
 181 pixel size options. While we are anticipating to obtain our SiPMs from the largest vendor,
 182 Hamamatsu, we are also characterizing SiPMs of similar pixel density and packing size from
 183 other vendors to ascertain whether they can fulfil our performance criteria for the LFHCal.
 184 All obtained SiPMs with their corresponding main characteristics can be found in Table 2, ac-
 185 cording to the vendors.

186 In order to verify the functionality of the SiPMs and to determine the spread of the break-
 187 down voltage, IV-curves were determined at ORNL and Yale for every SiPM using a Source-
 188 Measurement unit or PicoAmmeter and Voltage Source, respectively. Repeating the measure-
 189 ments at Yale allowed to verify the SiPM's and PCB's (Printed Circuit Boards) were not dam-

Table 2: SiPM types obtained with their characteristic features. Gain for Onsemi SiPMs given at $V_{bd} + 2.5$ V

| SiPM type | Vendor | size | pixel pitch | # pixels | fill factor | V_{bd} | opt. λ | PDE | Gain ($V_{bd} + 5$ V) | # tested |
|---------------|-----------|------------------------|-------------|----------|-------------|--------------------|----------------|-----|---------------------------|----------|
| S14160-1315PS | Hamamatsu | 1.3 cm \times 1.3 cm | 15 μ m | 7284 | 49% | (38 \pm 3) V | 460 nm | 32% | $3.6 \cdot 10^5$ | 5 |
| S14160-3015PS | Hamamatsu | 3 cm \times 3 cm | 15 μ m | 39984 | 49% | (38 \pm 3) V | 460 nm | 32% | $3.6 \cdot 10^5$ | - |
| S13360-1325PE | Hamamatsu | 1.3 cm \times 1.3 cm | 25 μ m | 2668 | 47% | (53 \pm 5) V | 450 nm | 25% | $7.0 \cdot 10^5$ | - |
| S13360-3025PE | Hamamatsu | 3 cm \times 3 cm | 25 μ m | 14400 | 47% | (53 \pm 5) V | 450 nm | 25% | $7.0 \cdot 10^5$ | - |
| S4K33C0115L | Broadcom | 3 cm \times 3 cm | 15 μ m | 38400 | - | (29.5 \pm 1.0) V | 430 nm | 29% | $7.0 \cdot 10^5$ | 9 |
| S4K33C0135L | Broadcom | 3 cm \times 3 cm | 35 μ m | 7396 | - | (29.5 \pm 1.0) V | 430 nm | 41% | $40.0 \cdot 10^5$ | 12 |
| S4K33C0147L | Broadcom | 3 cm \times 3 cm | 47 μ m | 4096 | - | (29.5 \pm 1.0) V | 430 nm | 44% | $70.0 \cdot 10^5$ | 2 |
| MICROFC-10010 | Onsemi | 1 cm \times 1 cm | 10 μ m | 2880 | 28% | (24.5 \pm 0.3) V | 420 nm | 18% | $2.0 \cdot 10^5$ | 3 |
| MICROFC-30035 | Onsemi | 3 cm \times 3 cm | 35 μ m | 4774 | 64% | (24.5 \pm 0.3) V | 420 nm | 41% | $30.0 \cdot 10^5$ | 3 |

aged during their transportation from ORNL to Yale. The obtained data is fitted with a two component fit to determine the V_{bd} , as seen in Figure 5(a). As seen in Figure 5(b) the spread of the break down voltages for the different SiPM types is in agreement with the numbers provided by the vendors, except for those given for the S4K33C0115L, which showed a significantly lower V_{bd} and a larger spread.

Due to delays in the delivery some of the Hamamatsu SiPMs types (S14160-3015PS, S13360-1325PE, S13360-3025PE) could not yet be tested. The corresponding evaluations will follow once they are delivered.

For the tile lab-test setup a CAEN DT5202 [5] digitizer is used. After calculating the V_{bd} , characterizing the dark count rate at a given over voltages (V_{op}) with the staircase plot, and conducting the different readout component tests, the single photon spectrum (SPE) was then characterized for the SiPM's. For this a CAEN LED Driver was mounted atop the SiPM and the signal was read out using the digitizer unit. Figure 6 shows an SPE spectrum recorded using the CAEN LED Driver for different two SiPM types. The wiggles in the blue line correspond to different PE peaks and fitting them gives the ADC/PE rate (orange line).

This fit gives an equivalence of 99 ADC/PE for the SiPM S4K33C0147 at $V_{op} = 2$ V, while for the MicroFC-10010 it is 86 ADC/PE at $V_{op} = 2$ V. Similar measurements will be performed for all SiPM types as a function of V_{op} to cross check the expected gain parameters, given in the data sheets.

2.4 Optimization and Granularity of the LFHCal & Insert

During the review of the calorimeter by the project in Dec. 2022, the initial concept of the LFHCal using wave length shifting fibers was put into question, mainly because of its significant complications during assembly. Afterwards, we started implementing different geometry options within the ePIC software stack in order to evaluate their performance in terms of resolution as well as acceptance and η -, ϕ dependence of the reconstruction performance. We compared there different designs:

1. The standard LFHCal, just replacing the WLS fiber readout with SiPMs in each layer.
2. A 90 degree rotated option of the LFHCal, letting the absorber align with the z-axis of the experiment (GFHCal), but keeping a similar sampling fraction and readout-channel count.

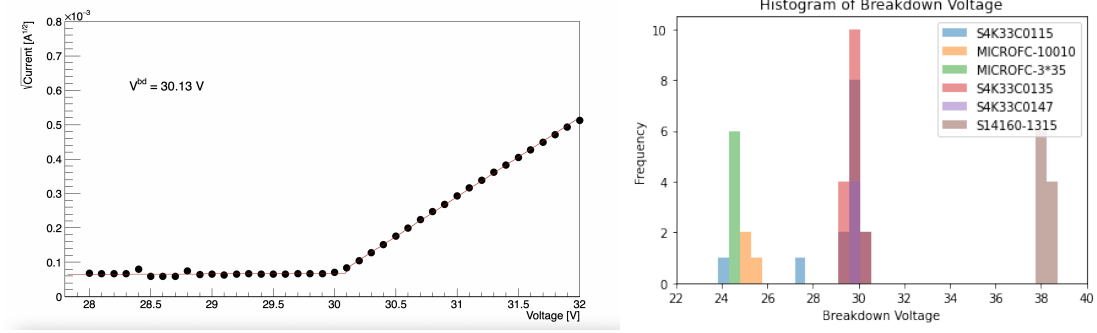


Figure 5: Left: IV Curve for SiPM S4K33C0147L. Right: Measured V_{bd} for all tested SiPMs.

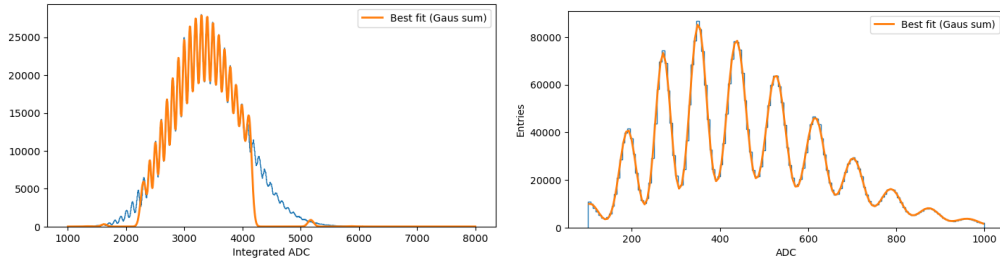


Figure 6: Single Photon spectrum (SPE) (blue histogram) together with its fit (orange line) for the SiPM S4K33C0147 ($V_{op} = 2$ V, left) and MicroFC-10010 ($V_{op} = 2$ V, right).

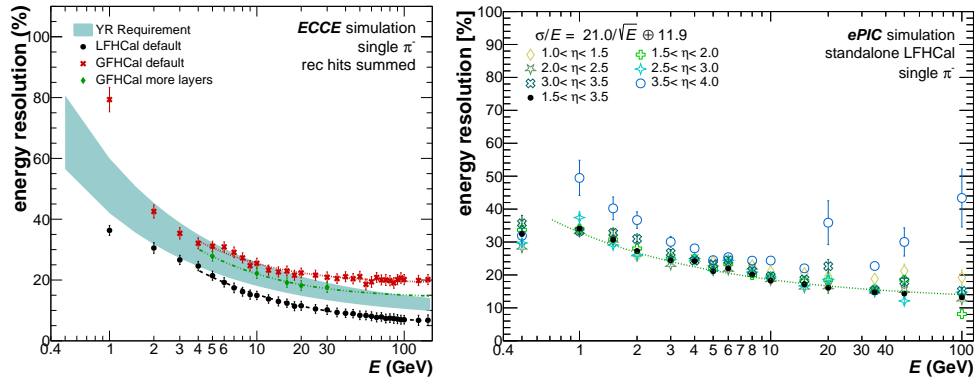


Figure 7: Resolution studies for different geometries (left) and η regions (right).

220 3. A 90 degree rotated option of the LFHCal, letting the absorber align with the z-axis of
 221 the experiment (GFHCal, increased π layers) with increased number of layers.

222 The obtained energy resolutions without material in front of the detector can be found in
 223 Figure 7 (left). Based on these studies it has been concluded that rotated design would yield a
 224 significantly worse performance especially above and below the beam pipe as well as at higher
 225 η . Thus the design was rejected and the decision was taken to follow the LFHCal design with
 226 buried SiPMs in each layer.

227 Further studies of the η dependence of the resolution close to the beam pipe (Figure 7 (right))

228 in combination with the inaccessibility of the SiPMs and scintillator tiles after construction,
229 yielded the inclusion of the insert into the baselined forward HCal design. Further studies
230 on the exact granularity needed for the insert are, however, still pending. The SiPM-on-tile
231 design for the LFHCal also allows to determine at a later stage the exact needed granularity
232 in the longitudinal direction, as the reading out more or less layers would primarily affect
233 the number of H2GCROCs needed per module and the summing boards. In order to address
234 some of these concerns ORNL hosted an EIC calorimetry workshop in April 2023, which
235 focused on the implementation of realistic geometries and reconstruction algorithms for all
236 calorimeters within ePIC. Moreover, first attempts at machine learning based clusterization
237 algorithms were developed during this workshop, which are being further explored during a
238 similar workshop for graduate students at the end of July in Germany.

239 **3 Remaining R&D Needs FY24**

240 **3.1 Scintillator Tiles**

241 Using the improved design of the LFHCal the challenges for the scintillator tile production
242 have shifted slightly compared to our original proposal. The proposed single tile geometry
243 should be easily feasible to produce both using machining as well as injection molding. Thus
244 the main concerns now are regarding the stability of the light yield and geometric tolerances in
245 both production processes and optimizing those at minimal cost. Consequently we are propos-
246 ing a systematic study of the influence of imperfections resulting from machining, as well as,
247 different machining processes and their long term impact on the stability of the light yield.
248 Using the machined tiles we would like to study the impact of different dimple geometries in
249 combination with the slightly different SiPM dimensions.

250 Similar studies will also be performed for the injection molded tiles, however, here only two
251 dimple geometries will be studied and the main free parameters are to be adjusted during the
252 injection molding process itself. In particular, controlling the cool-down process of the tiles as
253 well as their ejection from the mold can be studied in order to reduce geometric deformations
254 and thus keep the light yield stable within the same batch of tiles. Moreover, different raw
255 materials and dopants will be evaluated to maximize the light yield for the given geometry.

256 **3.2 Scintillator Characterization and Optimization**

257 All produced tile modules need to be characterized for their light yield, cross-talk and re-
258 sponse uniformity in order to validate the optimum machining and molding technique, whilst
259 minimizing the cost of the LFHCAL. Further optimization studies regarding the wrapping
260 and 8M-scintillator assembly will be performed. These initial characterization routines will
261 be important starting points to expand to a fully integrated quality assessment of each 8M-
262 scintillator assembly prior to integration into the full LFHCal 8M module. As part of this R&D
263 process we propose to develop a robust quality assurance procedure for single tiles, sheet as-
264 semblies as well as the full module. These procedures should included the characterization of
265 the scintillator tiles, assembled SiPMs and variations within the module layer to layer. More-
266 over, a first concept of the monitoring system of the LFHCal is needed, which can be used
267 during assembly, installation and operation to track the light yields in each tile, temperatures
268 and humidity within the calorimeter, as well as, the characteristics of the SiPMs.

269 3.3 Readout Electronics

270 Significant development work needs to be performed to design, implement and test read-
271 out electronics that can scale to all 90 000 channels of the combined pECAL/LFHCal system.
272 The requirements for the readout ASIC are low power consumption, to avoid active cooling,
273 and a very low noise while maintaining the large dynamic range required for the signals,
274 from a single MIP signal up to 200 GeV hadron showers. In addition, significant radiation
275 hardness of the ASIC is required closer to the beam pipe. For these requirements, we con-
276 sider the H2GCROCv3 developed for the CMS forward calorimetry upgrade at the LHC. The
277 H2GCROCv3 has 78 channels in total and a large dynamic range, from 0.1 fC to 10 pC, while
278 having a low power consumption of 20mW per channel. The dynamic range is achieved by
279 combining the 10-bit ADC (0 – 160 fC) and 12-bit TOT (160 fC – 10 pC).

280 The H2GCROC is controlled by fast commands and I2C protocol for slow control. It is
281 designed to work with the 40 MHz LHC clock (320 MHz for the fast commands and clocks).
282 Some R&D is needed to adopt the 40 MHz clock for the EIC needs, which will be developed on
283 an XILINX FPGA driving the ASIC. Each chip outputs 2 data links with a speed of 1.28 Gbps
284 and 4 trigger links which can be configured as a sum of 4 or 9 channels. The time measurement
285 of the 10-bit TOA is also read out via the data links. The data can then be connected to a FELIX
286 board, e.g. as used by sPHENIX, or other EIC specific readout units by optical links.

287 Since the larger topic of readout electronics and ASICs is treated in eRD109, no specific
288 request on R&D funds for the full forward calorimetry readout is made here. For the first
289 test beams with small-scale setups, we will be using a universal waveform sampling readout
290 system to obtain the largest possible amount of information from each channel. However, for
291 the foreseen common test beam between pECAL and LFHCAL in 2025 a close to final version
292 of a common readout board should be available, to exercise the full detector system.

293 Some electrical engineering expertise will be required to design the PCBs holding the SiPM
294 sensors in each layer as well as the signal transfer boards on the sides of the each module. Until
295 the final readout architecture is decided on, preliminary sensor boards do not necessarily need
296 to contain any complex electronics apart from the sensors, a bias voltage distribution and
297 potentially symmetric buffer amplifiers.

298 3.4 Prototypes and Test beams

299 The construction and testing of successively-larger R&D prototypes of the LFHCAL will be
300 important stepping stones towards the construction of the full LFHCAL system. It serves to
301 emphasize the expected performance numbers and to exercise all parts of the LFHCAL project
302 step-by-step, in order to build the needed confidence in the design required for a full scale
303 prototype.

304 First components of the LFHCAL will be taken to parasitic test beams at CERN during Septem-
305 ber and October 2023 in order to ascertain the saturation behaviour of the combined tile +
306 SiPM system by adding layers of absorber material between individual tiles and measuring
307 the individual and combined response of tiles to electromagnetic showers. In FY24 we plan to
308 follow up on these initial tests with one 8M module constructed out of the injection molded
309 tiles and another constructed using machined tiles. Once these campaigns have been con-
310 cluded successfully, we anticipate to have the necessary information to finalize all aspects of
311 the LFHCAL design and to construct an LFHCAL prototype on the lateral scale of 4 8M modules
312 and full depth, to be extensively tested in an extended test beam campaign together with a

313 similarly sized prototype of the pECAL. This combined full tower prototype module will be
314 equipped with the final pECAL/LFHCAL readout.

315 **3.5 Optimization of the Reconstruction Algorithms & Granularity of the** 316 **LFHCAL**

317 While significant progress has been made during the past year, regarding the geometry im-
318 plementation within the ePIC software stack the reconstruction software of the LFHCAL still
319 relies on a fairly simple clustering algorithm. This approach can recover the energy of single
320 particles hitting the calorimeter with a satisfactory energy resolution, however, it cannot cor-
321 rectly differentiate energy deposits within a jet from individual particles. Moreover, it cannot
322 yet correctly take into account the additional information encoded in the different longitudinal
323 segments. To further discriminate single particle within a high density environment we thus
324 would like to explore different machine learning algorithms to distinguish showers originating
325 from different particles. Including the HCal insert into our base line design for the LFHCAL
326 poses another challenge as its transverse granularity is different. Thus as part of this R&D
327 process, we plan to evaluate not only the optimum size of the tower front-face as a function
328 of the radial distance to the beam pipe for separation of particles within the jets but also its
329 depth segmentation in conjunction with the foreseen electromagnetic calorimeter and tracking
330 detectors to discriminate between different types of hadrons. In order to achieve this goal we
331 will be working towards a full particle flow algorithm in the ePIC forward region.

332 **4 Plans and Milestones for FY24**

333 In the following the R&D milestones and their respective expected deliverables are listed,
334 assuming a funding start of Oct. 2023

- 335 • **Tile production optimization using machining & injection molding (April 2024)**
 - 336 – Evaluation of different scintillator machining techniques and comparative review of
 - 337 different vendor capabilities regarding adherence to tolerances as well as optimizing
 - 338 the light yield and its stability for large number of tiles
 - 339 – Documentation of procedures for optimizing the light yield of injection molded tiles
 - 340 during the production process
 - 341 – High quality prototype tiles to equip two 8M modules for test beam studies
- 342 • **Reconstruction optimization (September 2024)**
 - 343 – Write-up of optimization results from simulations
- 344 • **Sensor board development (March 2024)**
 - 345 – First prototype of 8M-module-sized sensor board for Si-PM readout compatible with
 - 346 LFHCAL module geometry (together with eRD109)
- 347 • **Test module assembly (April 2024)**
 - 348 – First functional prototype of a full 8M module

349 • **Tile Characterization (August 2024)**

- 350 – Write-up of test bench & test beam measurement for all assembled tile-prototypes
 351 – First concept of a monitoring system to be installed in the LFHCaI

352 **4.1 Money Matrix**

353 The total funding requests broken down per institution and R&D activity can be found in
 354 Table 3 and 4, respectively. Time of students, postdocs and staff scientist for analysis of the
 various measurements is treated as contributed labor.

Table 3: Total funding request and breakdown by institution.

| institute | cost in FY24 k\$ | | | | total cost in FY23 k\$ |
|-----------|------------------|----------|-----------|--------|---------------------------|
| | eng. and tech. | material | equipment | travel | |
| ORNL | 13.0 | 20.0 | 0 | 5.0 | 38.0 |
| FNAL | 11.6 | 0 | 0 | 0.0 | 11.6 |
| Yale | 0 | 5.0 | 16.0 | 3.0 | 24.0 |
| Total | 24.6 | 25.0 | 16.0 | 8.0 | 73.6 |

355

Table 4: Total funding request by institution for each R&D activity.

| activity | cost in FY24 k\$ | | | total cost in FY24 k\$ |
|---------------------|------------------|------|------|---------------------------|
| | ORNL | FNAL | Yale | |
| Tile Production R&D | 15.0 | 11.6 | 5.0 | 31.6 |
| Tile Char. (Lab) | 0 | 0 | 19.0 | 19.0 |
| Sensor Board | 23.0 | 0 | 0 | 23.0 |
| Total | 38.0 | 11.6 | 24.0 | 73.6 |

356 **5 Plan for FY25-26**

357 CD2/CD3A end of FY23, from then on R&D shifts towards prototypes and project execution.
 358 R&D still necessary to answer open questions in time:

- 359 • Development and verification of robotic assembly stations, including fiber QA while
 360 laying, reproducibility etc.
- 361 • Development of QC procedures of finished tiles.
- 362 • Continuation of optimization of reconstruction algorithms with full EIC software
- 363 • Continued mechanical engineering support
- 364 • FY25 common testbeam with ECAL for final characterization of the full detector system

365 Moreover a common test beam campaign together with the pECaI is foreseen for FY25 and
 366 FY26 in order to obtain the final characteristics for the full detector system.

Table 5: Estimated funding requests for LFHCAL R&D efforts in FY25-26.

| Task | Estimated cost in \$ per year | |
|------------------------|--------------------------------------|-------------|
| | FY25 | FY26 |
| mechanical engineering | 30K | 20K |
| electrical engineering | 30K | 20K |
| materials | 40K | 40K |
| test beam support | 10K | 10K |
| total | 110K | 90K |

367 **A Appendix**

368 **B Detailed Funding Allocation for R&D in FY24**

Table 6: Funding allocation and approximate completion dates for respective milestones for FY24.

| Institute | Item | Cost per item in \$ | Number of items | Total cost in \$ | To be compl. by |
|---------------|--|---------------------|-----------------|------------------|-----------------|
| | Tile Production R&D: | | | | Q2/2024 |
| ORNL | cast material | | | 15K | |
| FNAL | raw material + dopant | | | (in kind) 0K | |
| FNAL | injection molder setup + operation | 180/h | 64h | 11.6K | Q4/2023 |
| ORNL/UTK/Yale | tile assembly | | 40h | (in kind) 0K | Q1/2024 |
| ORNL | travel | | | 5K | |
| | Tile Characterization (Lab Bench): | | | | Q3/2024 |
| Yale | scintillator material characterization | | 100h | (in kind) 0K | Q1/2024 |
| Yale | source measurement unit & led pulser, other material | 19K | 1 | 19K | |
| GSU/Yale/UCR | tile lightyield testing | | 160h | (in kind) 0K | Q3/2024 |
| Yale | travel | | | 3K | |
| | Sensor Board: | | | | Q1/2024 |
| ORNL | electrical engineering | 180/h | 72h | 13K | Q4/2023 |
| ORNL | connectors & cables | | | 5K | Q4/2023 |
| ORNL | sensor board production, assembly | | 160 | 5K | Q4/2023 |
| ORNL/UTK | testing | | 40h | (in kind) 0K | Q1/2024 |
| | Reconstruction Optimization: | | | | 2025 |
| UTK/Yale/BNL | simulations/digitization/reconstruction/analysis | | 640h | (in kind) 0K | |
| Total | | | | 73.6K | |

369 **B.1 Specific Expertise of Contributors**

370 **B.1.1 Oak Ridge National Laboratory**

371 The ORNL relativistic nuclear physics (RNP) working group is part of the ORNL physics
372 division. The RNP group has been, and continues to be, involved in the design, construction
373 and operation of the calorimeter systems of various collider based nuclear physics experiments
374 such as the STAR EMCal, PHENIX EMCal, ALICE EMCal as well as the proposed ALICE FoCal
375 upgrade. The RNP group is currently the main proponent of the LFHCAL proposal for EIC
376 detector one.

377 The contributions from the RNP group have made a significant impact on the design of
378 the ECCE calorimetry, tracking and PID systems from extensive studies based on detailed
379 simulations and full reconstruction codes. The results from these studies have shaped the
380 currently planned layout of EIC detector one to great extent. The mechanical design of the
381 LFHCAL has been supported by mechanical engineers from the ORNL nuclear fusion group.

382 At ORNL, the RNP group operates its own electronics laboratory currently housing test
383 setups for the sPHENIX MVTX streaming readout and slowcontrol. The RNP group owns sev-
384 eral modern 3D printers and has extensive experience in producing fast turnaround mechan-
385 ical mockups, which have been proven to be immensely helpful in designing the LFHCAL.
386 In addition, the RNP group has been granted access to a fully equipped electronics labora-
387 tory of the ORNL electronics and embedded systems group, which has extensive equipment
388 for climate controlled testing, silicon wafer probe stations, very fast oscilloscopes, optical test
389 benches etc.

390 Within the ORNL physics division, the working group of Mike Febraro is specialized in the
391 design, production and characterization of organic scintillator materials. This working group
392 has developed significant expertise in injection molding plastic scintillators for the LEGEND
393 experiment and also developed 3D printing capabilities for organic scintillator materials.

394 **B.1.2 Brookhaven National Laboratory**

395 Brookhaven National Laboratory is the host lab for the EIC project and has research groups
396 participating in many aspects of the EIC project and science efforts. In particular, the lab
397 made major contributions to the design and construction of the sPHENIX calorimeter systems
398 (EMCal and hadronic calorimeters). In both cases, the lab provided extensive mechanical and
399 electrical engineering support, and provided the assembly areas, both in the physics depart-
400 ment high bay areas, and nearby support buildings. BNL physics also provides a full comple-
401 ment of machine shops, detector labs and electronics labs, with many experienced engineers,
402 technicians and research staff supporting them.

403 **B.1.3 Fermi National Laboratory**

404 The Fermilab Detector R&D group has built extensive experience in extruding and injection
405 molding plastic scintillator materials used in various high energy physics experiments and
406 related fields. Their plastic scintillator production facility has capabilities to co-extrude large
407 plastic scintillator bars and to injection mold polystyrene based materials. Injection molding
408 has been successfully used to produce prototype voxel elements for the DUNE 3D scintillating
409 tracker detector (3DST) that will be part of the DUNE near detector complex. As part of the

410 CMS HGCAL project, the Fermilab group is currently exploring the possibilities to injection
411 mold small plastic scintillator tiles in large quantities.

412 B.1.4 Georgia State University

413 Dr. Megan Connors was a level 3 manager in the sPHENIX project responsible for
414 the Hadronic Calorimeter scintillator tiles.
415 The tiles were ordered from Uniplast (Russia) and tested at Georgia State University.
416 The tiles are made from extruded polystyrene with an embedded wavelength
417 shifting fiber. The two ends of the fiber exit at one location which is aligned with
418 an SiPM to measure the light collected. To test the performance of the tiles, GSU and
419 BNL designed a test stand that allowed to easily test thousands of tiles in batches of 8
420 at a time with cosmic rays. Two reference tiles were selected for each tile shape. These
421 reference tiles served as triggers during the tests and were placed on the bottom and top
422 of each stack of eight tiles. The ten tiles were
423 slid into the test stand that was composed of ten SiPMs on holders that aligned with the tiles,
424 which were read out with the CAEN DT5702 module. The ADC distribution was recorded
425 and the Most Probable Value (MPV) of each distribution was extracted in order to characterize
426 each tile with respect to the reference tile performance. Several studies were done to confirm
427 reproducibility and found that 30 minutes of collecting cosmic ray hits was sufficient for
428 determining the PR of the smaller inner tiles.
429
430
431
432
433
434
435
436

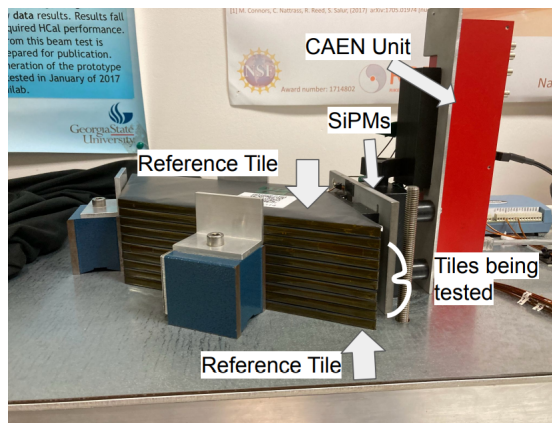


Figure 8: Test stand at Georgia State University for sPHENIX tile testing.

437 B.1.5 Iowa State University

438 The Iowa State Nuclear Experimental group has experience with trigger and data acquisition
439 electronics with the PHENIX experiment as well as electromagnetic calorimetry with the
440 MPC-EX detector (in PHENIX) and the hadronic calorimetry (in sPHENIX). Iowa State was
441 responsible for the Global and Local Level-1 trigger systems in PHENIX, and managed the
442 production of the inner and outer hadronic calorimeters in sPHENIX. Iowa State has electronics
443 design and testing capabilities through collaborations with the Electrical Engineering
444 Department, as well as relationships with local machine shops that offer manufacturing capabilities.
445 The sPHENIX inner HCAL sectors were manufactured in Ames, IA.

446 B.1.6 University of Tennessee Knoxville

447 The University of Tennessee (UTK) group has experience with detector assembly and production,
448 testing, and maintenance. Resources include offices and large experimental laboratory spaces
449 in the UTK Science and Engineering Facility (SERF). This facility includes high bay areas and
450 loading dock access. The Physics Department has a full machine shop with experienced
451 technicians. UTK successfully performed specific assembly steps of for the production

452 of all the IROCs (inner readout chambers) for the recent ALICE-USA Barrel Tracker Upgrade
453 project. This involved attaching pad-planes and strong-backs to assembled aluminum frames
454 and performing leak test qualification of the assembled IROCs. In addition to this ALICE-USA
455 BTU project, the UTK group has participated in the detector assembly and subsequent detector
456 maintenance for the PHENIX MuID, sPHENIX MVTX, and ALICE EMCal projects.

457 **B.1.7 Yale University**

458 The Yale group made, and continues to make, major contributions to the assembly, testing,
459 calibration, installation and operation of the ALICE EMCal. The renovated Wright Lab at Yale
460 allows the group access to large detector test and assembly areas, professional and student
461 machine shop, CAD computers with latest versions of several design programs and prototyp-
462 ing shop with 3-D printers, a large water jet cutter, and a large laser cutter. Over the past
463 few months members of the group have put together a lab test area with a light-tight box,
464 test stand, PCB and tile holders and a CAEN digitizer module, and are gaining experience in
465 testing the SiPMs and tile characteristics. The group also has significant experience in creating
466 and tuning calorimeter reconstruction software and exploiting Machine Learning techniques.

467 **B.1.8 University of California, Riverside**

468 The UCR group has about 750 sf laboratory space and a 400 sf ISO 7 cleanroom, which is
469 hosts standard equipment including: fast oscilloscopes, full-waveform fast digitizers (DRS4
470 boards), pico-second UV laser, picosecond pulse generator, source-measuring units, low-noise
471 power supplies, function generators, frequency counters, rubidium frequency standard, LED
472 drivers, calibrated photo-diodes, various optomechanical elements, dark boxes, environmental
473 chamber, fully-equipped soldering stations, stereo microscope, FDM and resin 3D printers,
474 computers with CAD software etc. Several UCR students have recent experience character-
475 izing plastic scintillator tiles with SiPM readout, including with measurements of light yield,
476 uniformity, time resolution, and cross-talk using radioactive sources, UV laser, and cosmic
477 rays. UCR has a fully equipped machine shop capable of small production runs at a subsidized
478 rate (36 dollars per hour).

479 **B.1.9 Valparaiso University, Valparaiso**

480 The experimental nuclear and particle physics group at Valparaiso University (Valpo) has been
481 active for more than 30 years and has participated in experiments including MEGA (LAMPF
482 E969), NuSea (FNAL E866), the Crystal Ball (BNL-AGS E913), TWIST (TRIUMF E614), nEDM
483 experiments at NIST and (currently) at LANL and ORNL, and the STAR experiment at RHIC.
484 The faculty, staff, and undergraduate students at Valparaiso have been engaged in physics
485 analysis, and also often in detector construction and operation. For STAR, components of the
486 Endcap Electromagnetic Calorimeter (EEMC) were constructed at Valparaiso and we played
487 a role in calibration, particle reconstruction, and an ongoing role in physics analysis with
488 the EEMC. More recently, undergraduates from Valparaiso were involved in refurbishing the
489 PHENIX sampling EMCal to become the STAR Forward Calorimeter System (FCS) EMCal. The
490 slow controls software for the FCS was written at Valparaiso, and almost 10,000 scintillation
491 tiles were polished, painted, and packaged at Valparaiso and recently installed in the FCS
492 HCal.

493 **References**

- 494 [1] F. Bock, et al., Design and Simulated Performance of Calorimetry Systems for the ECCE
495 Detector at the Electron Ion Collider (7 2022). [arXiv:2207.09437](https://arxiv.org/abs/2207.09437).
- 496 [2] A. Laudrain, on behalf of the CALICE Collaboration, The calice ahcal: a highly granular
497 sipm-on-tile hadron calorimeter prototype, Journal of Physics: Conference Series 2374 (1)
498 (2022) 012017. doi:10.1088/1742-6596/2374/1/012017.
499 URL <https://dx.doi.org/10.1088/1742-6596/2374/1/012017>
- 500 [3] The Phase-2 Upgrade of the CMS Endcap Calorimeter, Tech. rep., CERN, Geneva (2017).
501 doi:10.17181/CERN.IV8M.1JY2.
502 URL <https://cds.cern.ch/record/2293646>
- 503 [4] R. Abdul Khalek, et al., Science Requirements and Detector Concepts for the Electron-Ion
504 Collider: EIC Yellow Report (3 2021). [arXiv:2103.05419](https://arxiv.org/abs/2103.05419).
- 505 [5] A5202/DT5202 64-Channel Citiroc-1A Unit for FERS-5200.